Numerical Modeling of Air Mass Trajectories from the Biomass Burning Areas of the Amazon Basin

SAULO RIBEIRO DE FREITAS[1], KARLA MARIA LONGO[1], MARIA ASSUNÇÃO F. SILVA DIAS[2] and PAULO ARTAXO[3]

[1]Centro Universitário de Palmas, Universidade do Tocantins
[2]Departamento de Ciências Atmosféricas, Instituto Astronômico e Geofísico, Universidade de São Paulo, Rua do Matão, 1226, Cidade Universitária, 05508-900 São Paulo, SP, Brasil
[3]Departamento de Física Aplicada, Instituto de Física, Universidade de São Paulo

Manuscript received on March, 1996; accepted for publication on October 30, 1996

ABSTRACT

The dry season in Central Brazil and Amazonia (from June to October) is characterized by intense biomass burning whose emissions are a major source of greenhouse gases and aerosol particles. In order to study sources, sinks and destination, Three Dimensional Air Mass Trajectories were calculated from source regions in the case where a north-bound mid-latitude cold from approaches southern Brazil. Two examples are shown: July 1993 and August 1995. The method of determining 3D air mass trajectories is based on a limited area atmospheric model with high resolution of 20 km in the area where the trajectories start, and a lower resolution of 80 km elsewhere. For the 1995 case only the coarser resolution grid is used. The model is nudged at every timestep towards a global analysis available every 12 hours. It was observed that the approaching cold front provides a conveyor belt where sloping ascent of the 3D trajectories takes place. This movement transport gases and aerosol particles up to upper troposphere. This long range transport of gases and aerosol particles may have a significant climate impact in the southern hemisphere.

Key words: biomass burning, trajectories, global change, Amazon.

INTRODUCTION

The dry season in Central Brazil and Amazon Region, from June to October, is characterized by intense biomass burning (Crutzen & Andreae, 1990). Large gas and aerosol particles emissions have been detected and reported by several authors (Andreae *et al.*, 1988; Kirchhoff *et al.*, 1985, 1991; Setzer & Pereira, 1991; Artaxo *et al.*, 1993, 1994, 1995; Setzer *et al.*, 1994). These studies discuss the local impacts and the possibility of long range transport of pollutants which could have a continental or even an hemispheric impact.

Correspondence to: M.A.F. Silva Dias

The transport of atmospheric pollutants, either in a regional scale or in a long range perspective, depends basically on the atmospheric structure of turbulence and winds which will disperse and advect the air mass, respectively. Kirchhoff *et al.* (1991) included in their discussion and interpretation of local measurements of ozone and carbon monoxide in southeastern Brazil the possible origin of the sampled air mass through the determination of isobaric air mass trajectories. Inspite of the limitations on the isobaric approach restricted to a single level, they concluded that ozone enhancements were consistent with the origin of the air mass traced by backward trajectories towards the Central and Western regions of Brazil.

In the specific case of the air circulation in the dry season in Amazon and in Central Brazil, the possible air mass trajectories still present an open problem. From the climatology point of view, Central Brazil is dominated from June to September by a high pressure area with little precipitation and very slow wind speeds at lower levels (Riehl, 1979). However, on a day to day basis, the transient phenomena represent perturbations that may lead to a quite different picture. The approach of mid latitude fronts from the south as reported by Kousky & Ferreira (1981) and Fortune & Kousky (1983) produce a disturbance on the atmospheric stability and on the wind field. From the North, the propagating squall lines originated at the northern coast of Brazil (Silva Dias & Ferreira, 1992; Cohen *et al.*, 1995) present another perturbation typical of the dry season. Moreover, local circulation induced by topography in Central Brazil and by the Andes mountains (*c.f.* Fig. 1) may provide another disturbance to the climatological set up.

Whenever one of these perturbations is acting in the area of interest, or in its proximity, the three dimensional wind field structure is affected and vertical advection becomes important. The wind field over the area in higher levels is prone to having higher wind speeds thus enhancing the long range transport of pollutants. The three dimensional air mass trajectories should therefore be examined in different atmospheric situations. This paper will focus on two examples of long range transport of pollutants through the direct interference of approaching mid latitude cold fronts.

THE METHOD OF AIR MASS TRAJECTORY CIRCULATION

The 3D trajectories were determined from the wind fields generated by the Regional Atmospheric

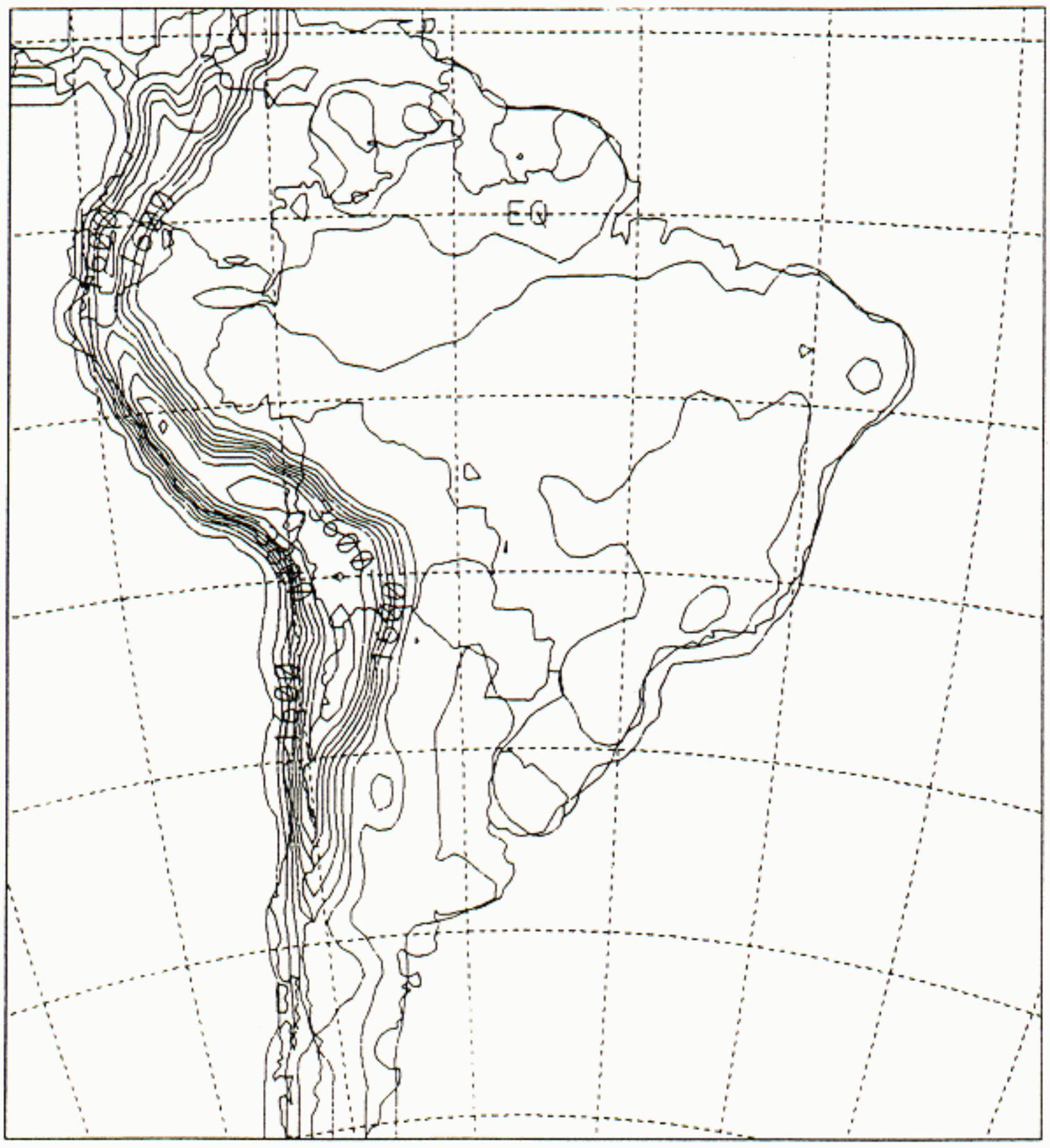

Fig. 1 — Topography of South America. Isolines start at 100m above sea level and increase by 250m.

Modeling System – RAMS model described by Tripoli & Cotton (1982) and Pielke *et al.* (1992). The model is run in a three dimensional version with a larger scale grid of 80 km resolution covering most of South America and neighboring Atlantic ocean. From the 1993 case study, a nested grid with 20 km resolution is located over Central Brazil and most of Amazon to provide a better description of the low level wind field. The model vertical resolution starts at 100m in lower levels stretching at a rate of 1.2 up to 1200m and then keeping a constant resolution up to model top located at 15.5 km. The physical parametrizations included are the anisotropic turbulence dependent on the deformation tensor, atmospheric long and short wave radiation interacting with water vapor and liquid water, surface interaction including the effect of vegetation, input from a soil model, and the effect of deep cumulus clouds and cloud microphysics. The details of these parametrizations may be found in the references of Pielke *et al.* (1992). The simulations are carried out from an initial condition provided by the interpolation of the National Centers for Environmental Prediction – NCEP – 2.5 degree analysis. The model is nudged at every time step towards the NCEP analysis, available at every 12 hours, at the boundaries and model top and in a lesser extent but still important at the model center. In this way the simulation can be carried out for several days and the simulated wind field reproduces the large scale features of the observed flow depicted in the NCEP analysis. The three dimensional simulated wind fields are stored at every 2 hours of simulation and are the input to the trajectory computation.

The method to determine the 3D trajectories is based on the equation $\frac{d\vec{r}}{dt} = \vec{v}[\vec{r}(t)]$ with an initial value $\vec{r}(t_0) = \vec{r0}$, where $\vec{r}$ is the position in space at time t and $\vec{v}$ is the three dimensional velocity field. Petterssen (1956) suggested a recursive method to solve the trajectory equation to obtain $\vec{r}$ at all times from $\vec{v}$. The position at a future time is calculated from the starting position wind speed vector. The future position is then recalculated from an interpolated wind speed vector, between the initial position and the future position calculated in the previous iteration. This recursive method stops when convergence is achieved. Seibert (1993) discusses the numerical aspects of this scheme and shows that the numerical solution is accurate to the second order.

RESULTS AND DISCUSSION

The first example to be discussed is the period from 12 to 19 July, 1993. Figure 2 a,b shows, respectively, the NCEP analysis for the 14 July 1993, 00 UTC, at 850 hPa (approximately 1500m Above Sea Level – ASL) and 17 July 93, 00 UTC, at 300 hPa (≈ 9500m ASL). Figure 2c shows the METEOSAT satellite infrared – IR – image at 14 July – 01 UTC. The main feature depicted by the satellite image is the cold front which according to Figure 2a extends from a low pressure area at 30°S, 45°W, reaches the coast at 23°S and extends northwestward towards Central Brazil. On July 13, the front intersection with the coast line was about 3 degrees further south (not shown); the front remained almost stationary up to July 16 and then moved east. Figure 2d shows the main burning areas in Amazon and Central Brazil obtained from the NOAA-11 3.7 μm IR channel for July 12. The positions indicated in Figure 2d were used as the starting position for the forward air mass trajectory calculations. The vertical level were trajectories start was varied from 50 to 500m above ground level without significant difference in the results. This insensitivity to the starting level is due basically to the strong vertical mixing in the boundary layer during the daytime period.

Figure 3 shows the ensemble of 3D air mass trajectories from the starting points in Figure 2d. Figure 3a shows all trajectories while Figures 3b,c,d show a few representative trajectories with the label indicating height in meters ASL; the time difference between dots along the trajectory is 24 hours. It may be seen that 3D air mass trajectories start moving towards the west and upwards; upon reaching western Amazonia between 2000 and 4000m ASL, they start turning southward (responding to the anticyclonic flow at 700 hPa, not shown) and, further along turn to southwest and still upward. The sloping ascent is in the form of a

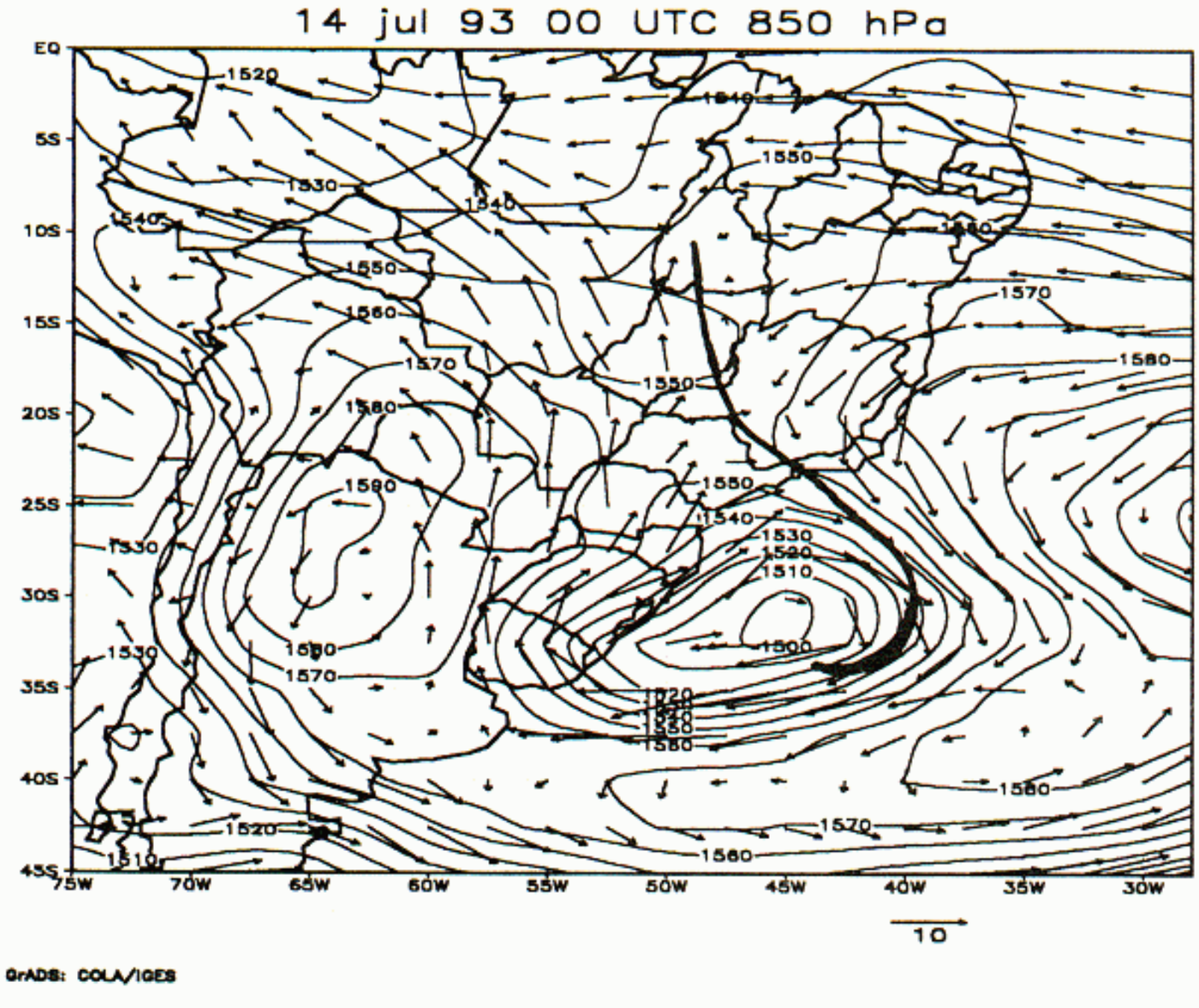

a

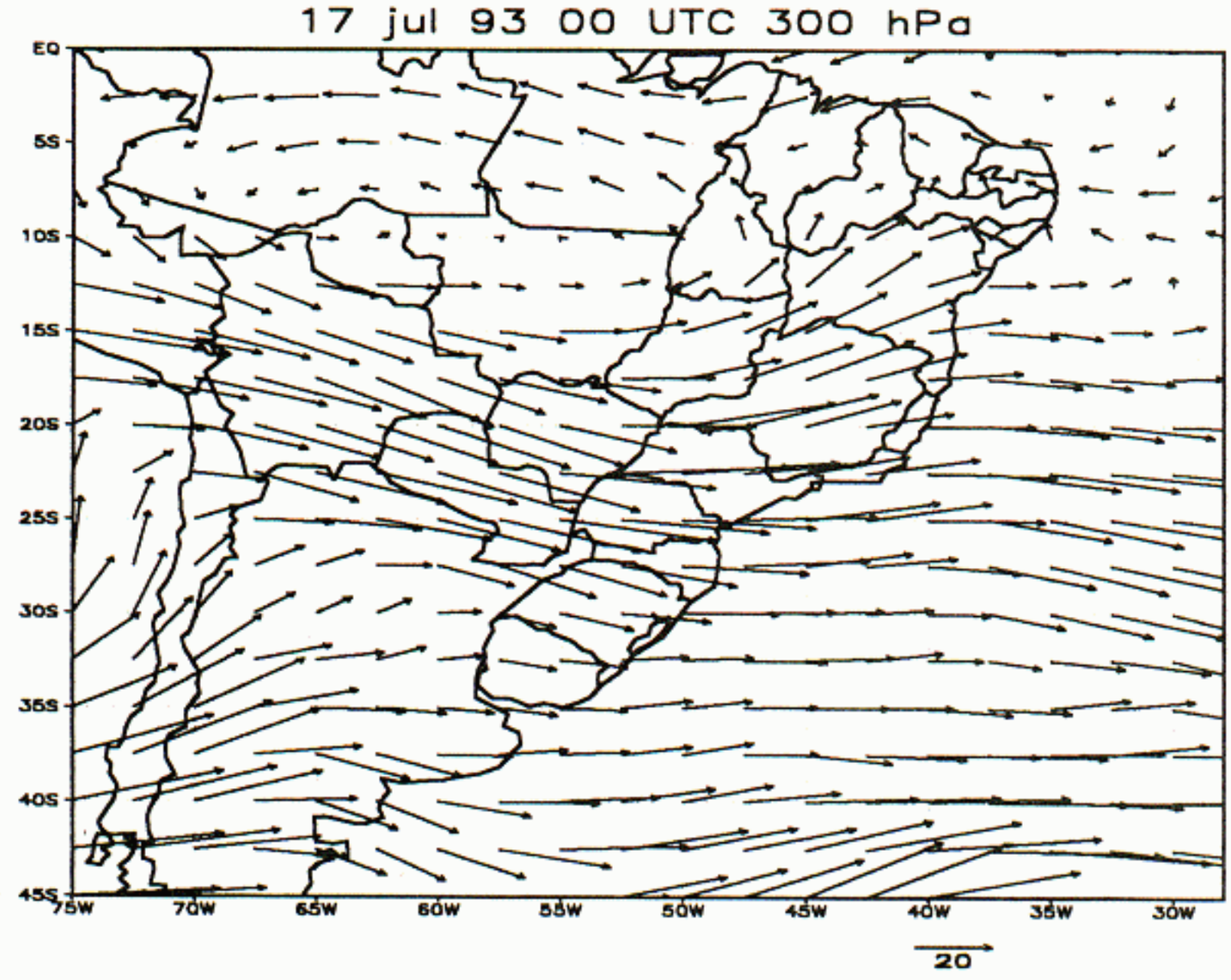

b

Fig. 2 — (a) Wind and geopotential field at 850 hPa for July 14, 1993 at 0 UTC (size of the arrow indicates wind speed in $m.s^{-1}$ and over the Andes the fields are graphically interpolated); (b) wind field at 300 hPa for July 17, 1993 at 0 UTC (size of the arrow indicates wind speed in $m.s^{-1}$); (c) METEOSAT-5 IR image for July 14, 1993, 01 UTC; (d) burning spots for July 12, 1993 based on NOAA-11 IR images (obtained from A. Setzer).

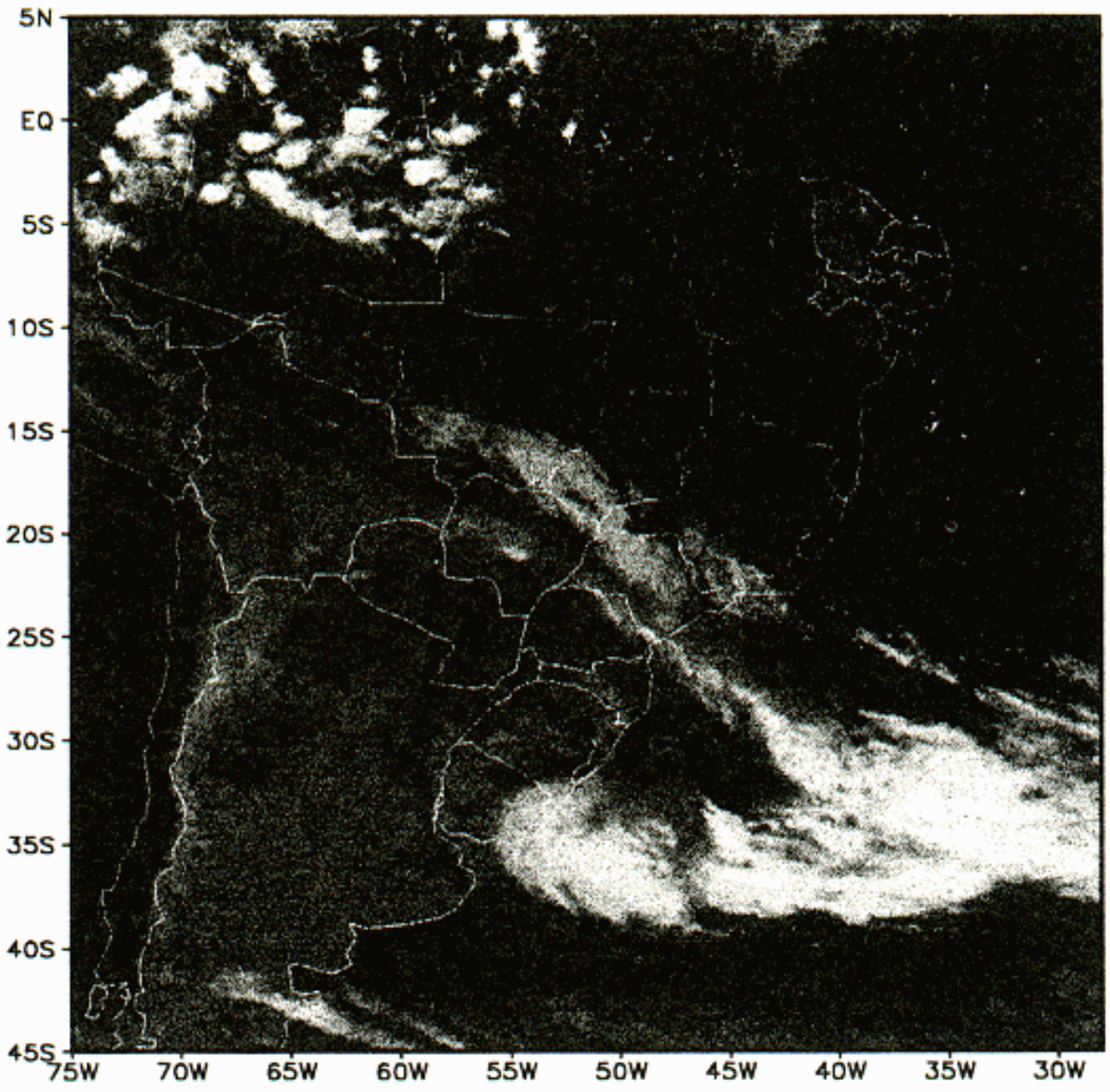

c

d

Fig. 2 (Continuation).

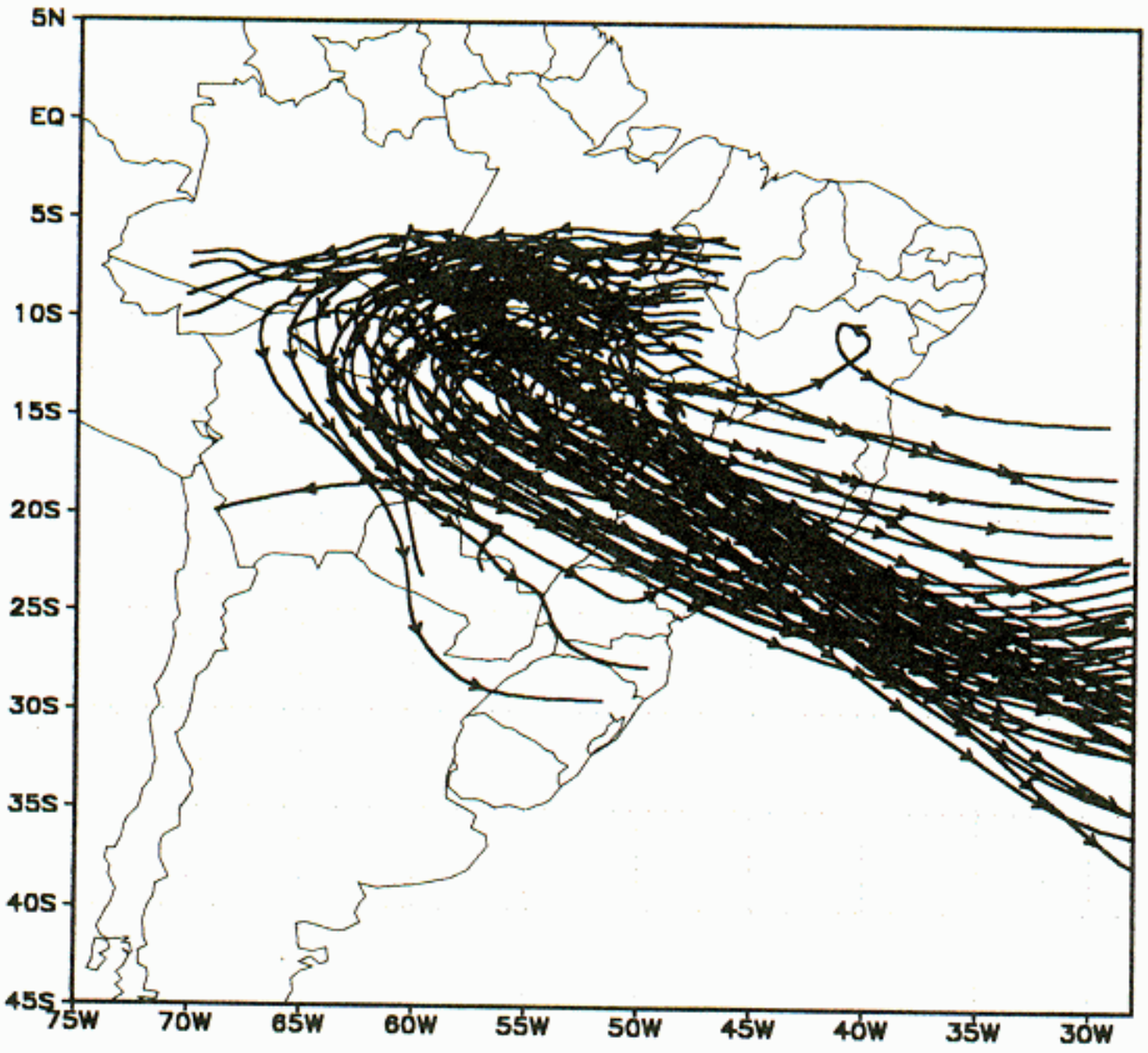

a

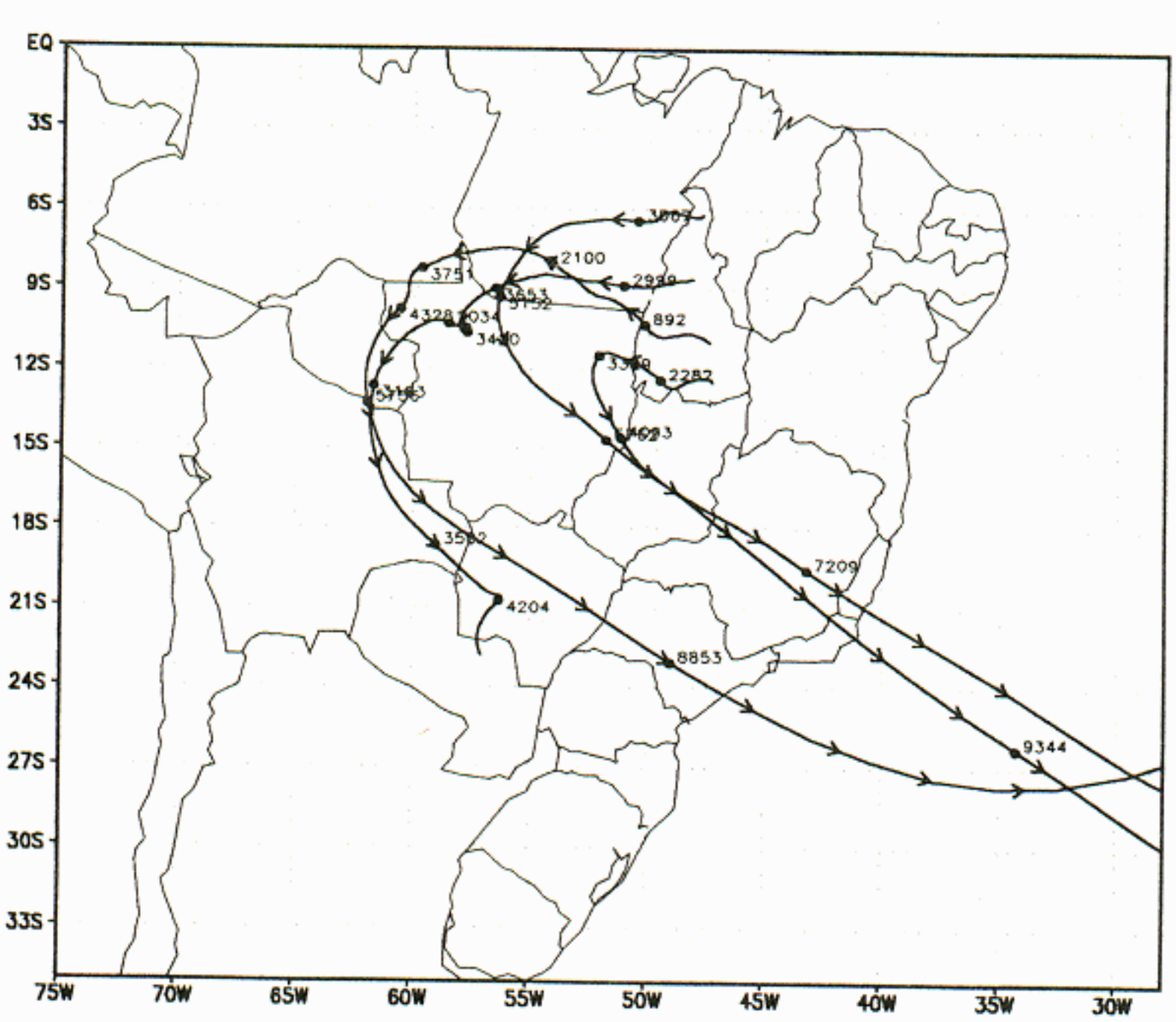

b

Fig. 3 — (a) Trajectory ensemble starting from the burning spots in Figure 2d; (b) a few trajectories starting in the state of Tocantins; the time difference between dots is 24 hours and the labels represent height ASL in meters; (c) same as (b) for the state of Mato Grosso; (d) same as (b) for the state of Goiás.

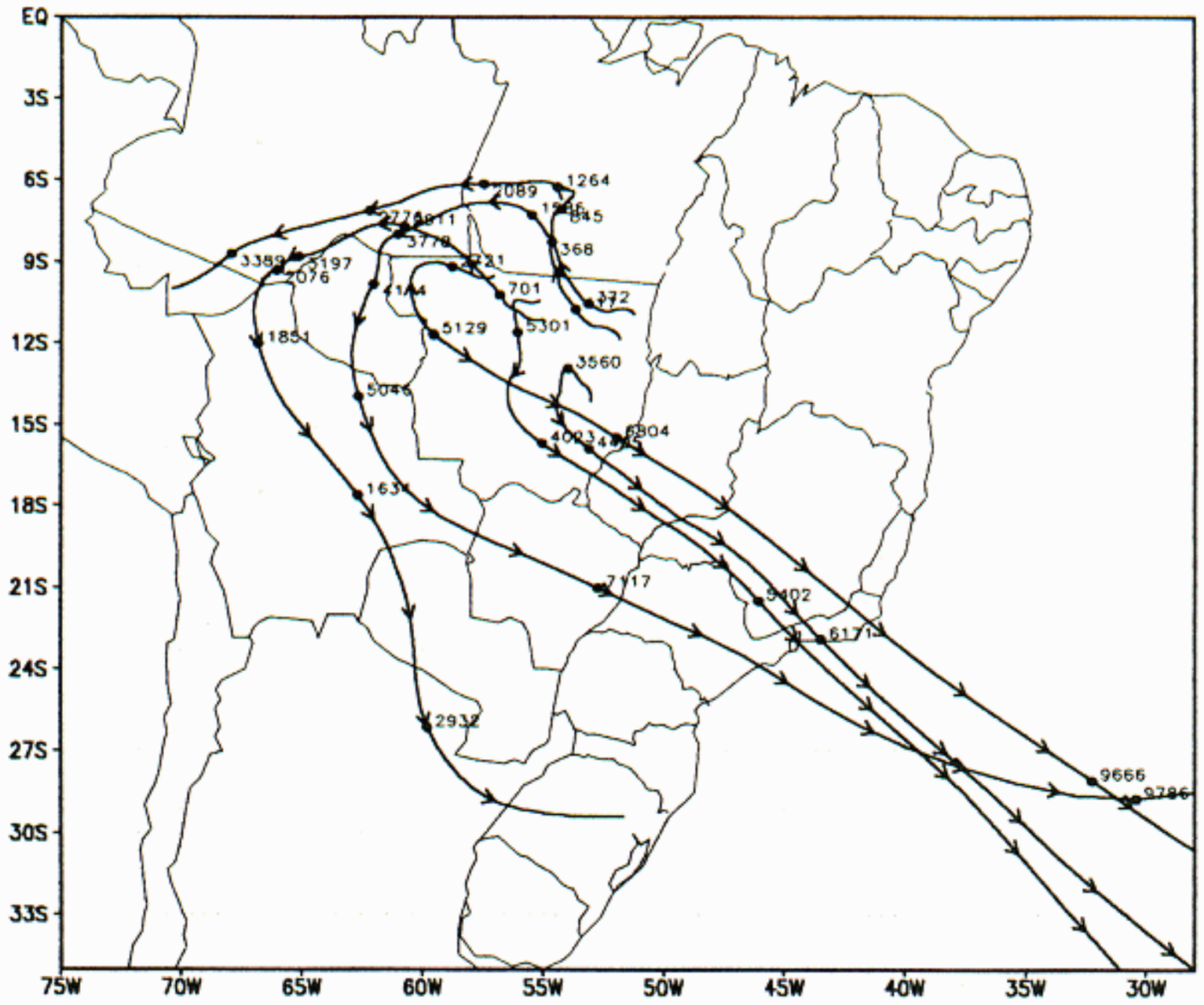

c

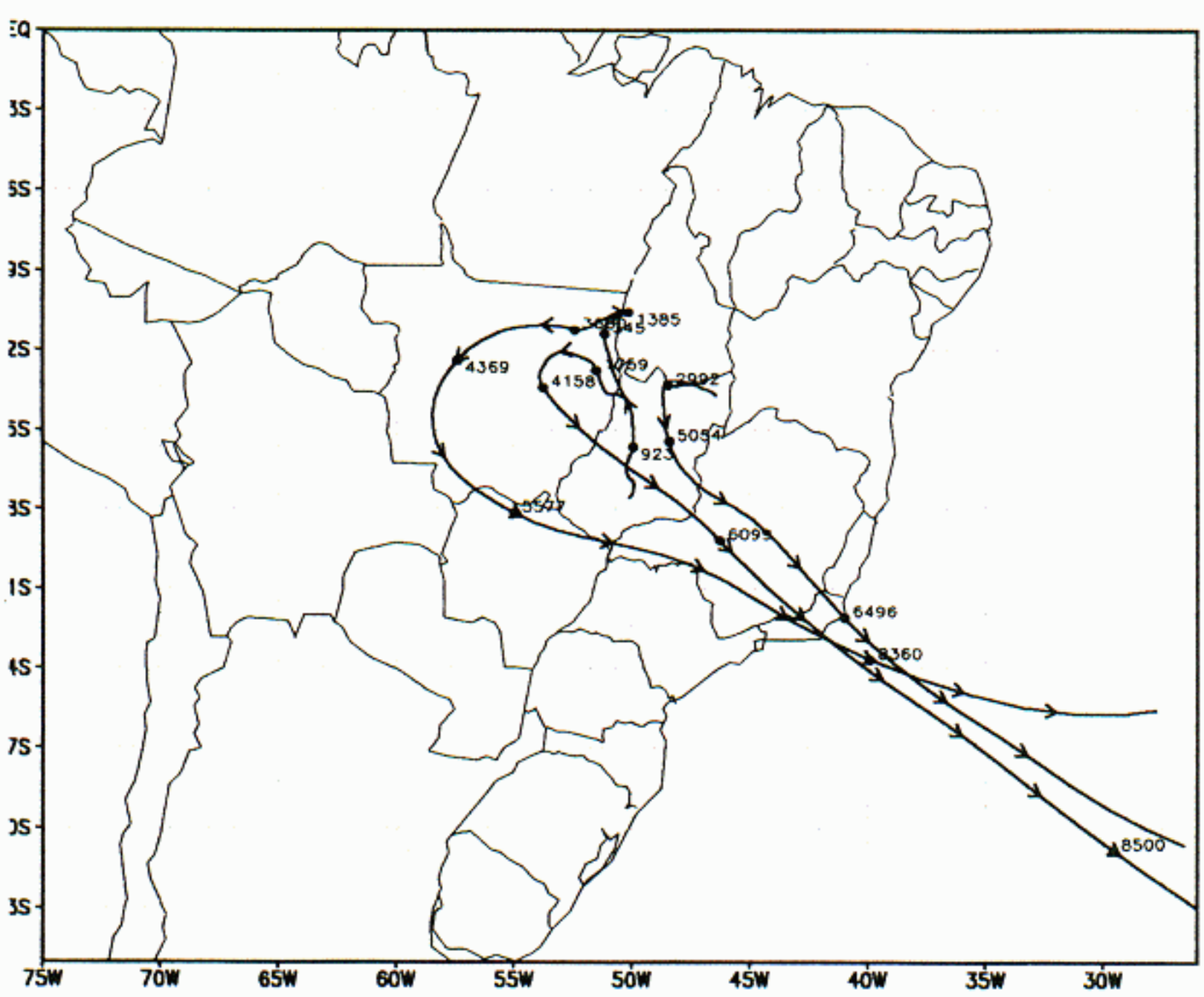

d

Fig. 3 (Continuation).

conveyor belt that reaches high altitudes at 6000 to 9000m ASL in the southern Atlantic. Figure 3c shows that the 3D air mass trajectories that move further west in the beginning actually succeed in avoiding the conveyor belt produced by the cold front; the air parcels then move further south towards northern Argentina and at about 300m ASL, turn to the east, cross southern Brazil at about the same height. Trajectories which start at about 10°S 52°W move initially northward and then westward; their progress is much slower than for the ones that turn to south and to southeast since the latter reach subtropical latitudes and higher levels where they encounter higher wind speeds (*c.f.* Fig. 2b). Figure 4 is similar to Figure 3 but the starting time of the trajectories is July 13, at 00 UTC, with the burning spots from the satellite image of July 13 (not shown). Although the same general features are found in this case, a few differences are noticeable. Figure 4b has a trajectory starting at 8°S 47°W which moved upwards quite fast and ended up after 6 days over the tropical Atlantic along 11°S and at about 12000m ASL. As the cold front remained in a quasi stationary position from July 14 to 16, the sloping ascent of the air mass in the conveyor belt persisted as the most permanent feature of this period.

Throughout the whole simulation, Central Brazil showed no convective clouds. A few convective clouds were present in the simulation (not shown) and in the satellite image (Fig. 2c) in the northwestern part of Amazonia. The trajectories that move towards western Amazonia may be affected by clouds. However, the model does not have enough resolution to resolve convective scale transports of air parcels; what the convective parametrization induces is an enhanced large scale upward motion forced by local convective heating, which will turn the trajectories upward but with a velocity much smaller than the one inside convection. This is surely a shortcoming of the present approach and should be addressed in a future work through the introduction of nested grids in convective areas. In the present case, convective transports along the cold front ascent may be considered negligible since no deep convection was observed along its inland portion.

The second example discussed is the period from August 22 to 29 1995, during the SCAR-B (Smoke Clouds and Aerosols – Brazil) mission. Figure 5a shows the burning spots for August 23 from the GOES-8 4 μm IR image, and Figure 5b shows the GOES-8 corresponding visible image with the indication of smoky regions for August 29. Figure 6a,b shows the wind field at 850 hPa for August 26, 12 UTC and at 500 hPa (≈ 5500m ASL) for 12 UTC August 28, respectively. A cold front may be seen in Figure 6a extending from a low pressure area at 35°S, 62°W towards northern Argentina.

The 3D air mass trajectories from the burning spots of Figure 5a are shown in Figure 6c,d. In this case, two categories of trajectories are clearly defined. A first group of trajectories start north of about 10°S and move upwards and westwards crossing over the Andes after 5 days. A second group starts south of 10°S and then move southward, reach the conveyor belt associated with the cold front, go up to 3000m ASL just south of Paraguay, turn towards the east, travel over southern Brazil still in a sloping ascent and finally reach more than 5000m ASL in the southern Atlantic along 30°S, in accordance with the wind field in Figure 6d, and also in about 5 days. Comparing the heights in Figure 6d with the topography heights in Figure 1, it may be seen that from the equator to 10°S, the trajectories remain at about 4500m ASL while the deepest montains seen by the 80 km grid have less than 3000m. This ascent is part of the local circulation in the boundary layer enhanced by the diurnal heating of the terrain. Ibañez (1995) had already pointed out this effect of the Andes in the local flow.

Comparing Figure 6C with Figure 5b it may be seen that there is a striking resemblance between the area indicated by the trajectories and the area covered by smoke. This fact shows that the 3D air mass trajectories correctly agree with the long range transport of biomass burning plumes. From this combined analysis of 3D trajectory analysis and satellite images it is clear that biomass

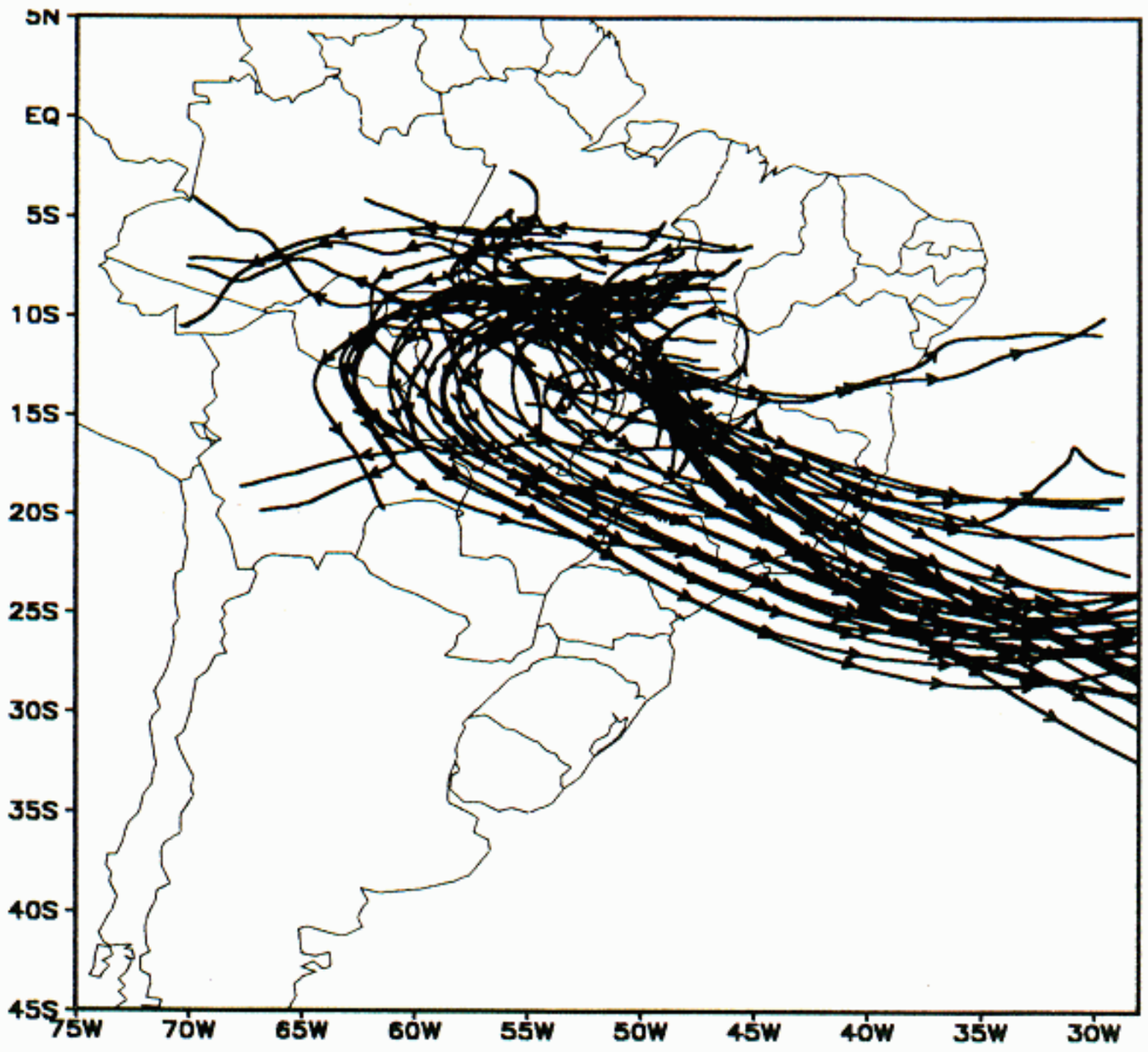

a

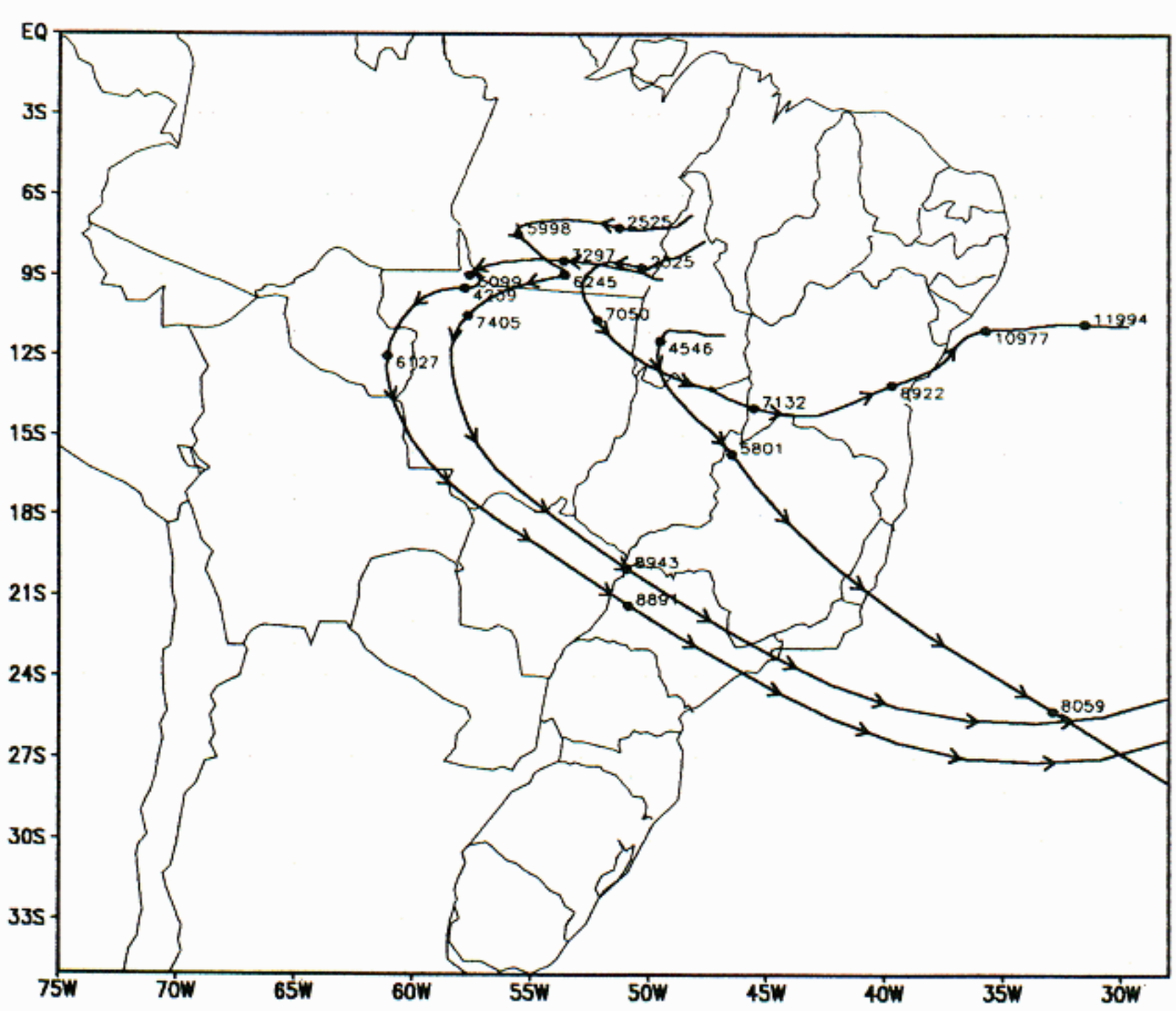

b

Fig. 4 — Same as figure 3 for the burning spots of July 13, 1993.

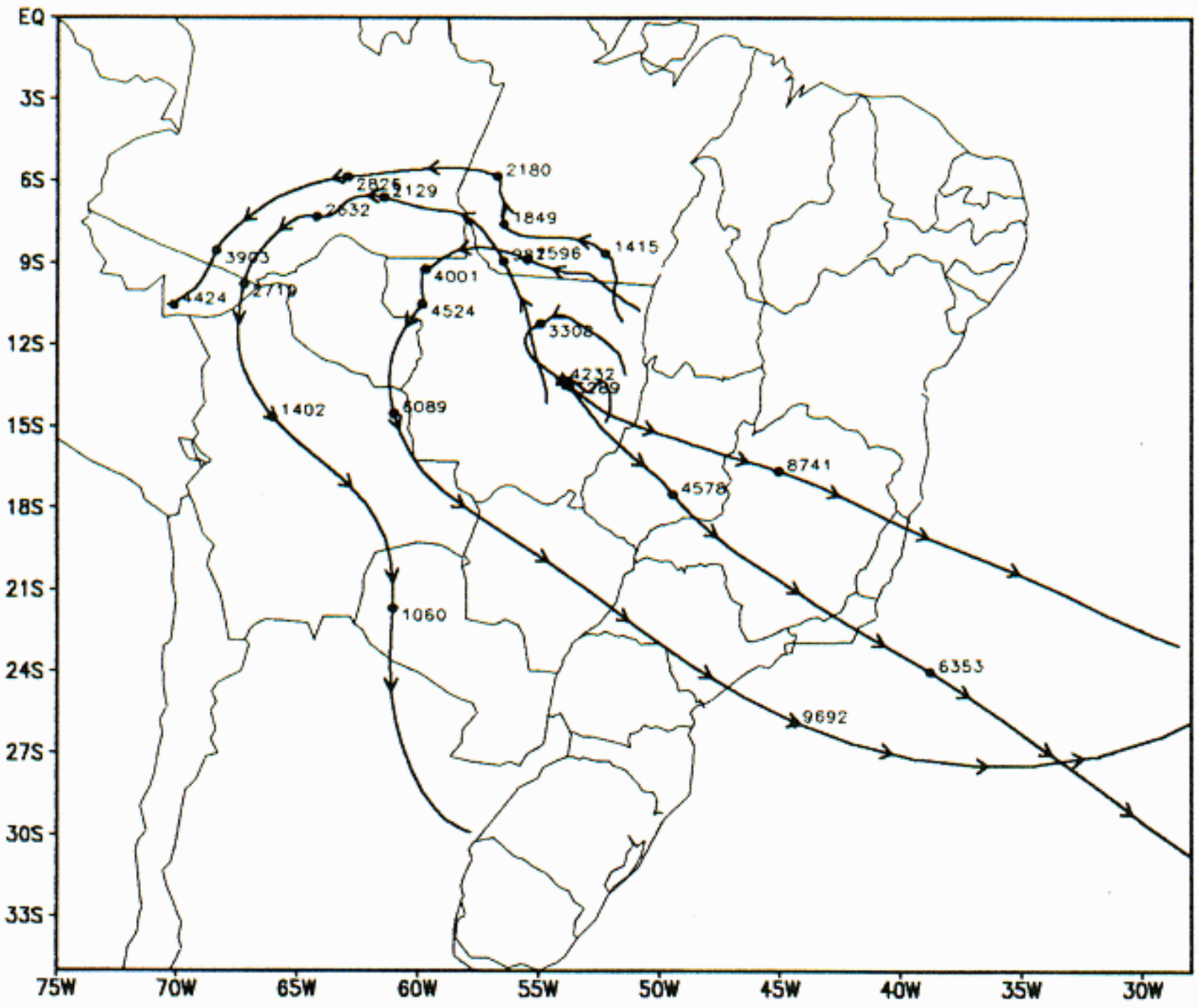

c

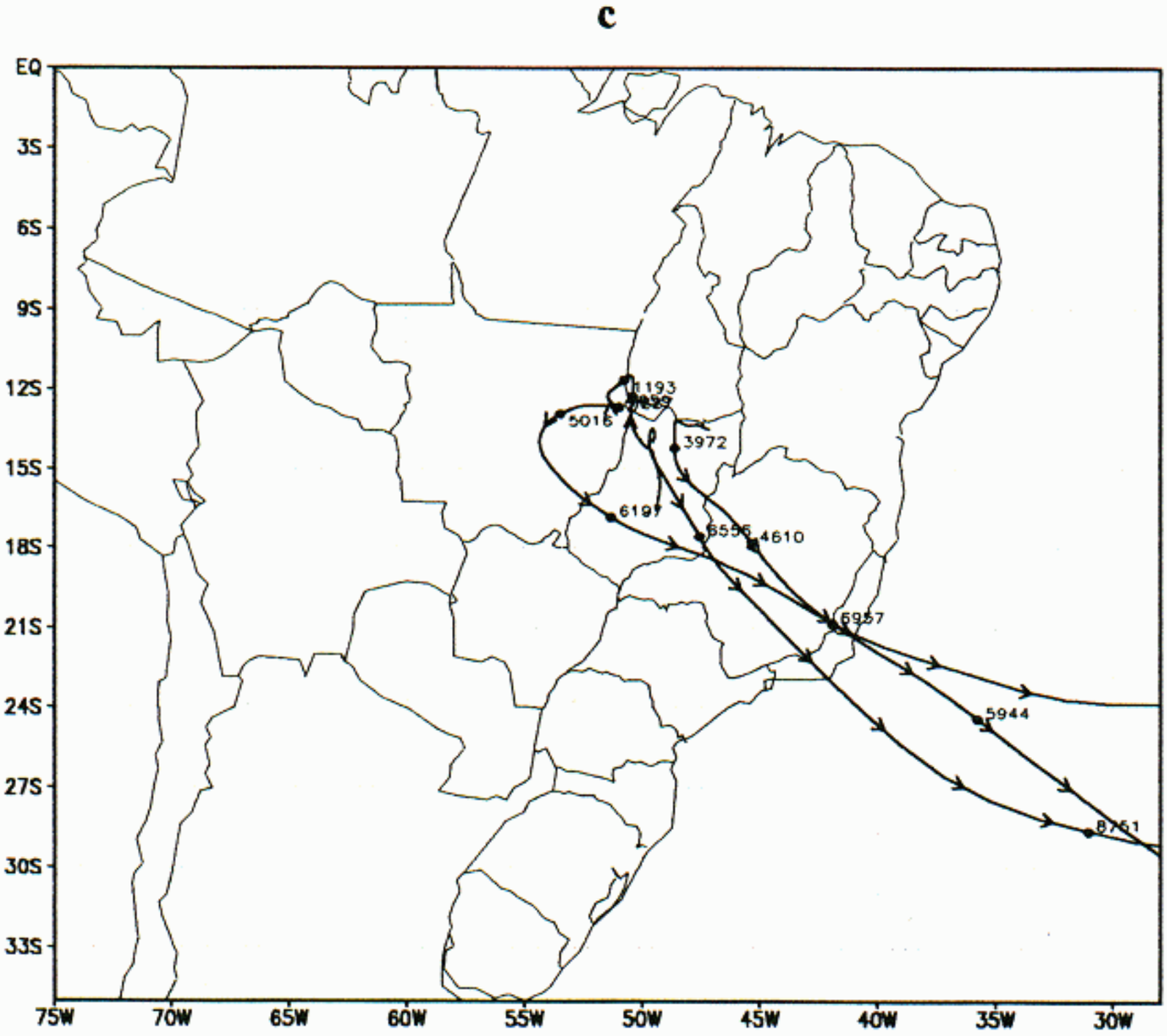

d

Fig. 4 (Continuation).

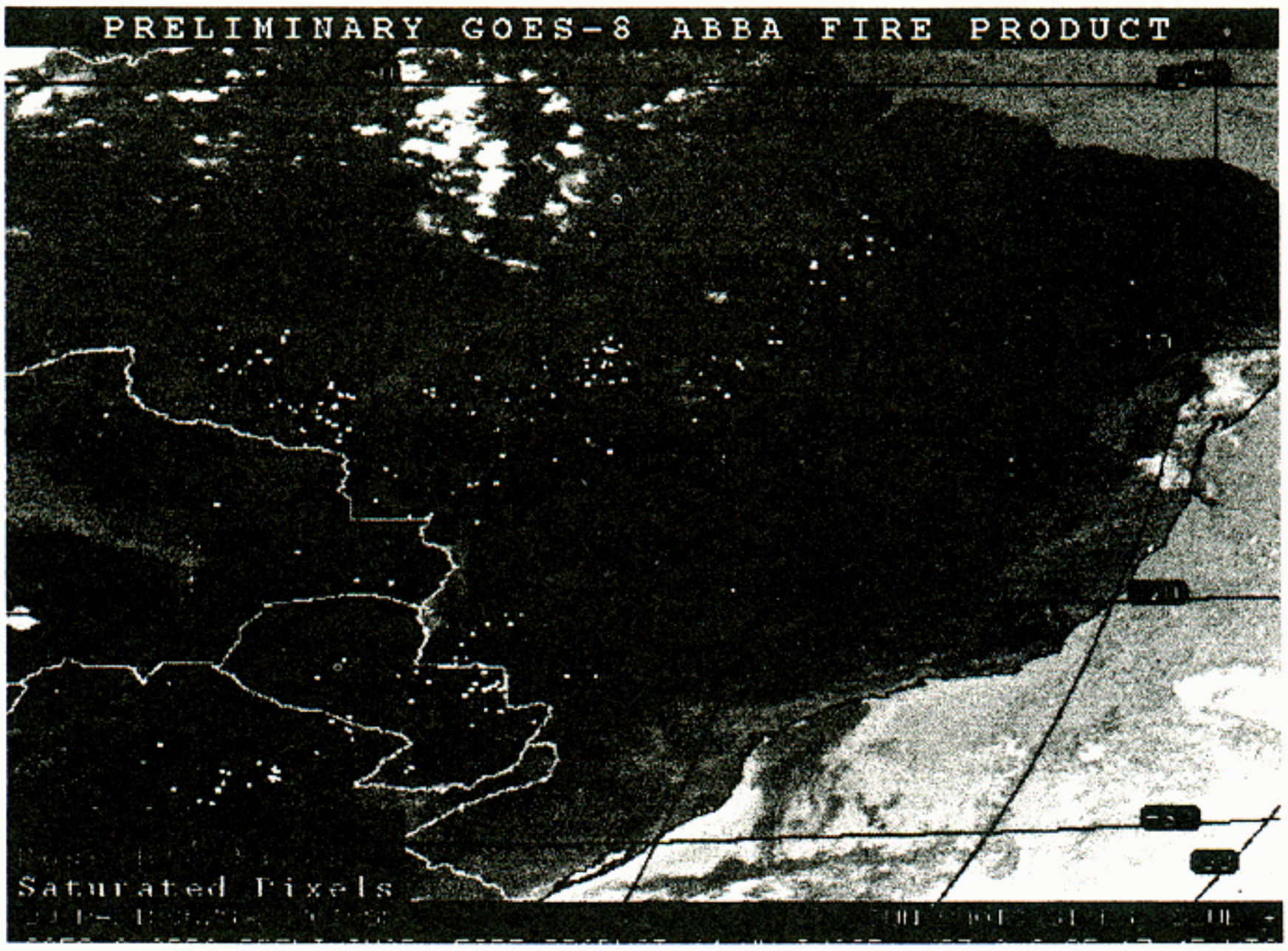

a

b

Fig. 5 — (a) GOES-8 IR image for August 23, 1994 showing the burning spots (white dots); (b) GOES-8 visible image for August 29, 1995, with the smoke analysis performed by the University of Wisconsin at Madison.

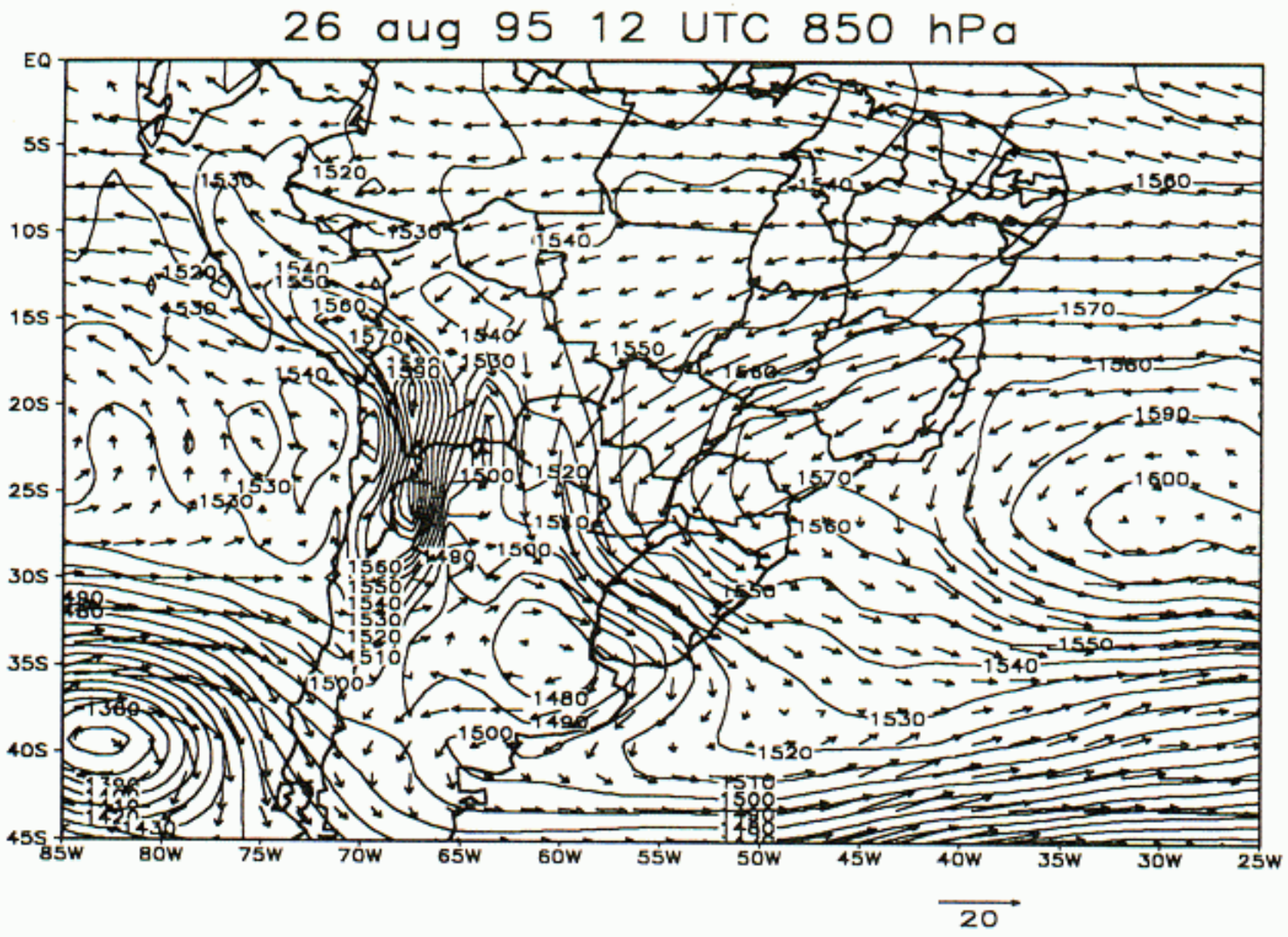

a

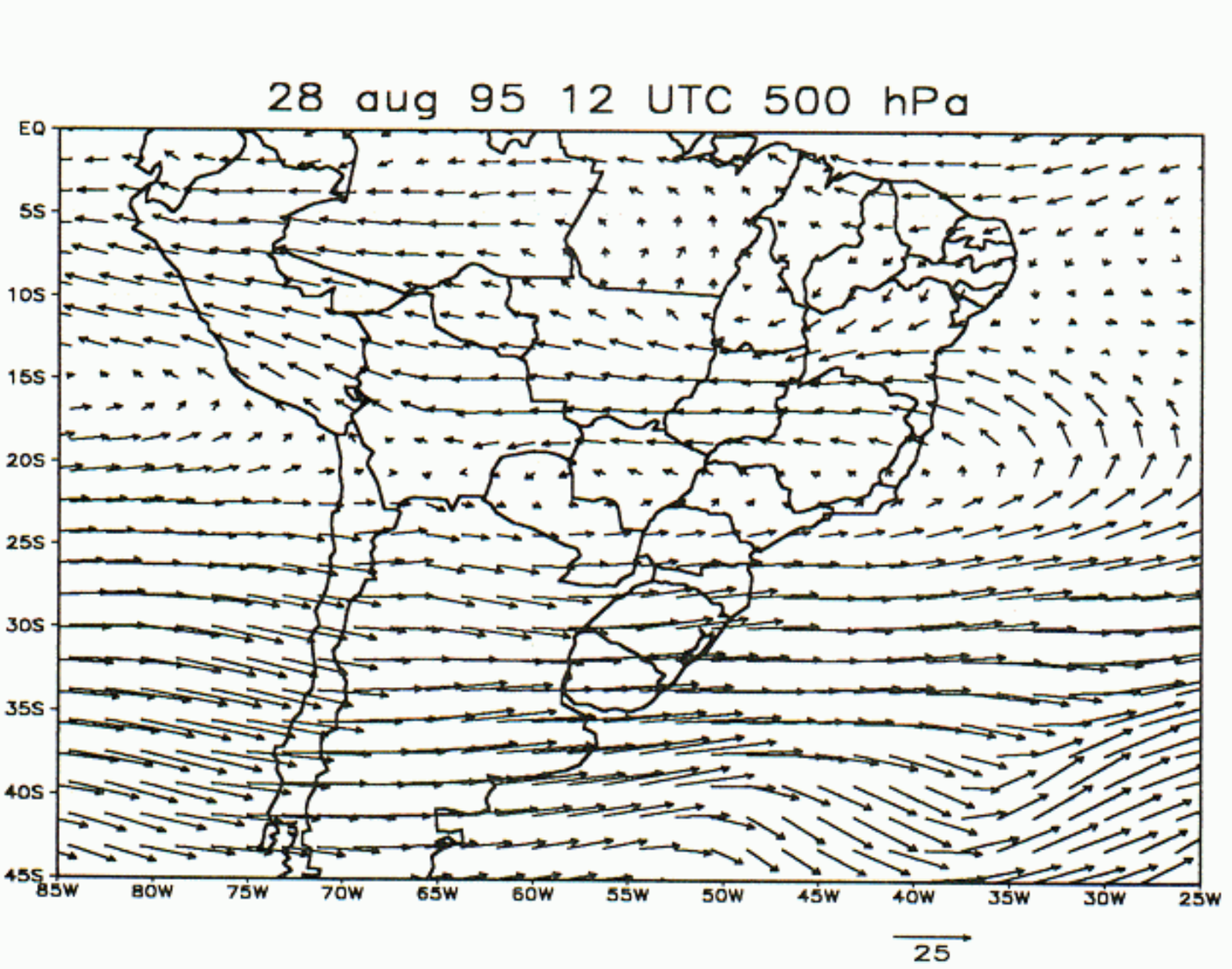

b

Fig. 6 — Wind and geopotential field at 850 hPA for August 26, 1995 at 12 UTC (size of the arrow indicates wind speed in $m.s^{-1}$ and note that over the Andes the fields have been graphically interpolated); (b) wind field at 500 hPa for August 28, 1995 at 12 UTC (size of the arrow indicates wind speed in $m.s^{-1}$); (c) trajectory ensemble starting from the burning spots in Figure 4a; (d) a few representative trajectories with labels as in Figure 3b.

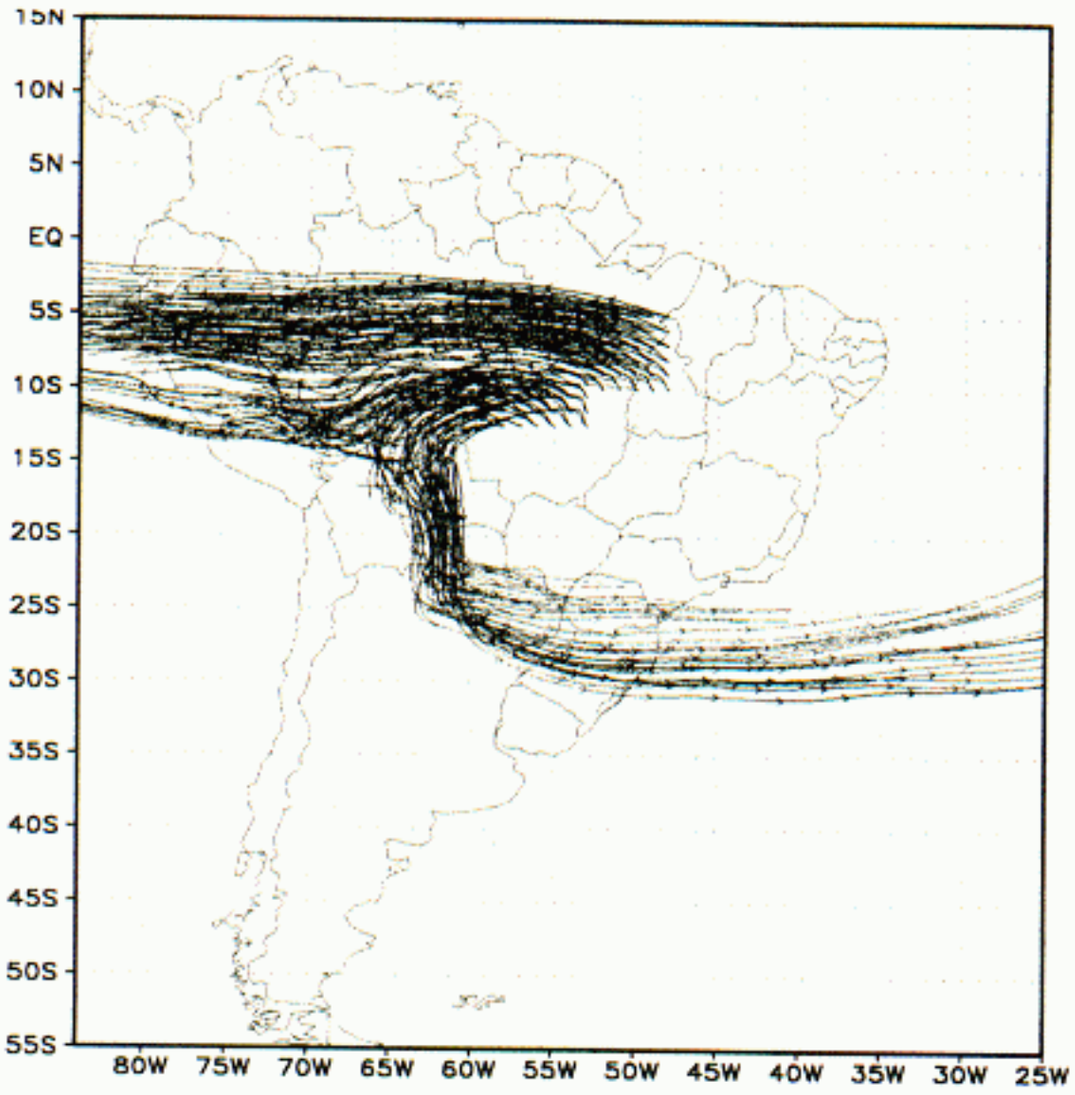

c

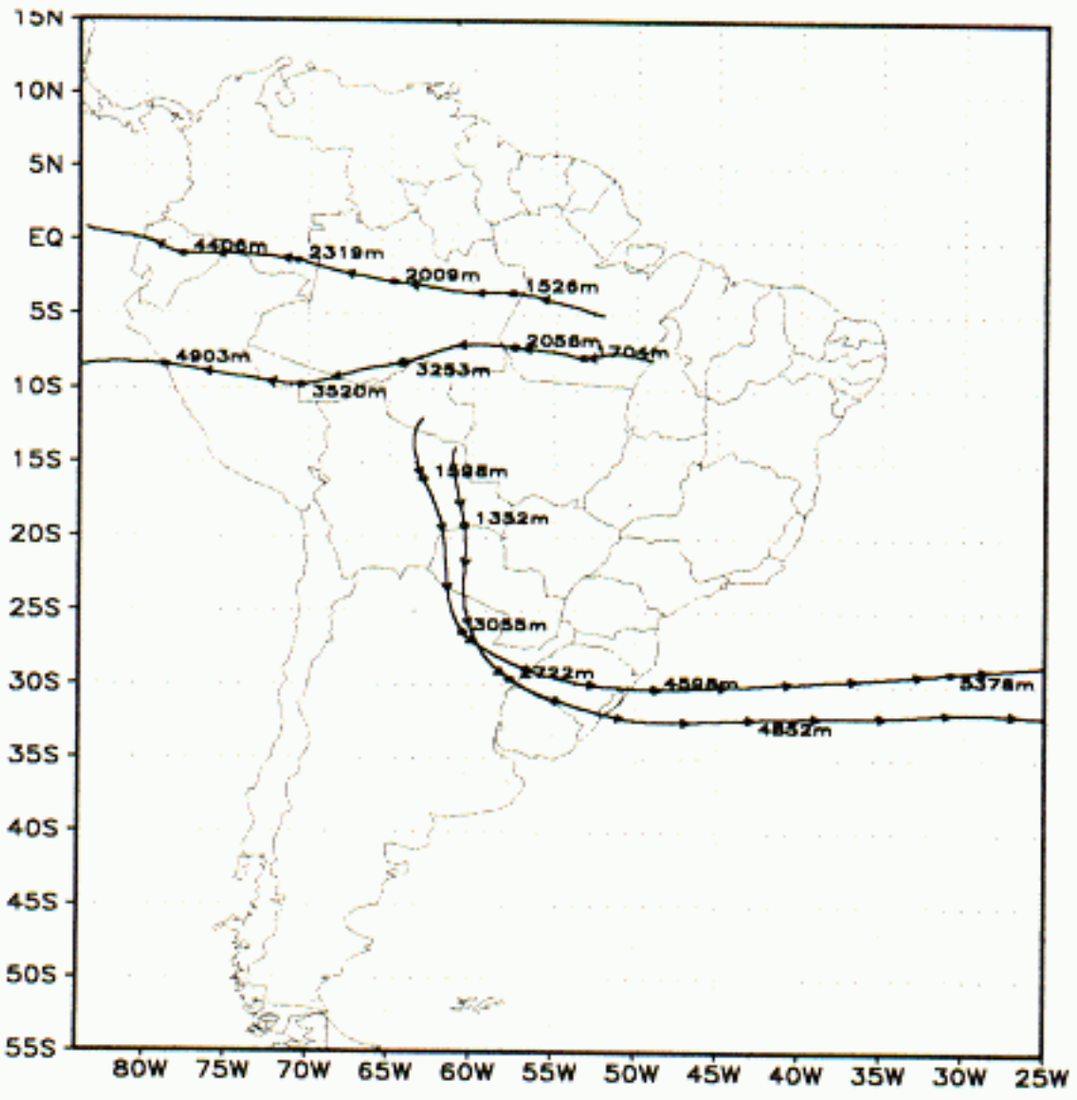

d

Fig. 6 (Continuation).

burning emissions strongly affected atmospheric characteristics over large areas of South America and the Southern Atlantic Ocean. The high aerosol loading in the troposphere affects the radiative balance of the atmosphere over large areas. One important result from these analyses is the indication of biomass burning emissions reaching high altitudes (6000-9000 meters ASL), where they can be transported over the South Atlantic Ocean. These air parcels enter the global circulation pattern, affecting the Southern Hemisphere atmospheric composition. Similar biomass burning emissions in Southern Africa, Southeast Asia (*e.g.* Malaysia, Thailand), and Australia affect the global atmospheric composition with additional effects that are still unknown.

ACKNOWLEDGEMENTS

We would like to acknowledge the data on burning spots obtained from Dr. A. Setzer/INPE for the dry season of 1993 and the processed and analyzed images of the IR and visible channels obtained from the University of Wisconsin at Madison for the SCAR-B period through E. Prince. The large scale analysis data is from NCEP. The RAMS code is licensed by ASTER, Inc. The figures have been drafted using GrADS from COLA. This research has been supported by FAPESP and CNPq.

REFERENCES

ANDREAE, M. O.; BROWELL, E. V.; GARSTANG, M.; GREGORY, G. L.; HARRISS, R. C.; HILL, G. F.; JACOB, D. J.; PEREIRA, M. C.; SACHSE, G. W.; SETZER, A. W.; SILVA DIAS, P. L.; TALBOT, R. W.; TORRES, A. L. & WOFSY, S. C., (1988), Biomass burning emissions and associated haze layers in Amazonia. *J. Geophys. Res.,* **93:** 1509-1527.

ARTAXO, P.; GERAB, F.; YAMASOE, M. A. & MARTINS, J. C., (1994), Fine Mode Aerosol Composition in Three Long Term Atmospheric Monitoring Sampling Stations in the Amazon Basin. *J. Geophys. Res.,* **99** (D11): 22857-22868.

ARTAXO, P.; GERAB, F.; YAMASOE, M. A. & MARTINS, J. C., (1995), The chemistry of atmospheric aerosols particles in the Amazon Basin. *In*: SEIDL, P. R.; GOTTLIEB, O. R.; KAPLAN, M. A. C., eds. *Chemistry of the Amazon: Biodiversity, natural products and environmental concerns*, American Chemical Society Books Series, ACS Symposium series 588, p. 265-280.

ARTAXO, P.; YAMASOE, M. A.; MARTINS, J. C.; LOCINAS, S.; CARVALHO, S. & MAENHAUT, W., (1993), Case study of measurements in Brazil: Aerosol emissions from Amazon Basin fires. *In*: CRUTZEN, P. J. & J.G. GOLDAMMER, ed. *Fire in the Environment: Its Ecological, Climatic and Atmospheric Chemical Importance*, Wiley & Sons, p. 139-158.

COHEN, J. C. P.; SILVA DIAS, M. A. F. & NOBRE, C. A., (1995), Environmental conditions associated with Amazonian squall lines: a case study. *Mon. Wea. Rev.*, **123** (11): 3163-3174.

CRUTZEN, P. J. & ANDREAE, M., (1990), Biomass burning in the tropics: impact on atmospheric chemistry and biogeochemical cycles. *Science,* **250:** 1669-1678.

FORTUNE, M. & KOUSKY, V. E., (1983), Two severe freezes in Brazil: precursors and synoptic evolution. *Mon. Wea. Rev.*, **111:** 181-196.

IBAÑEZ, J. D., (1995), *Influência dos Andes nas circulações locais do Peru* (Master Thesis IAG-USP).

KIRCHHOFF, V. W. J. H.; SAHAI, Y. & SILVA DIAS, P. L., (1985), Medidas de ozônio a bordo do avião Bandeirantes do INPE. *Revista Brasileira de Geofísica,* **4** (1): 21-26.

KIRCHHOFF, V. W. J. H.; MARINHO, E. V. A.; DIAS, P. L. S.; PEREIRA, E. B.; CALHEIROS, R. V.; ANDRÉ, R. & VOLPE, C., (1991), Enhancements of CO and O_3 from Burnings in Sugar Cane Fields. *J. Atmosph. Chemistry,* **12:** 87-102.

KOUSKY, V. E. & FERREIRA, N. J., (1981), Interdiurnal surface pressure variations in Brazil: their spatial distribution, origins and effects. *Mon. Wea. Rev.*, **109:** 1999-2008.

PETTERSSEN, S., (1956), *Weather Analysis and Forecasting*, vol. 1, McGraw Hill, 428p.

PIELKE, R. A.; COTTON, W. R.; WALKO, R. L.; TREMBACK, C. J.; LYONS, W. A.; GRASSO, L. D.; NICHOLS, M. E.; MORAN, M. D.; WESLEY, D. A.; LEE, T. J. & COPELAND, J. H., (1992), A comprehensive meteorological modeling system – RAMS. *Meteor. Atmos. Phys.,* **49:** 69-91.

RIEHL, H., (1979), *Climate and Weather in the Tropics.* Academic Press, 611p.

SEIBERT, P., (1993), Convergence and accuracy of numerical methods for trajectory calculations. *J. Applied Meteor.,* **32:** 558-566.

SETZER, A. W. & PEREIRA, M. C., (1991), Amazon biomass burning in 1987 and an estimate of their tropospheric emissions. *Ambio,* **20:** 19-22.

SETZER, A. W.; PEREIRA, M. C. & PEREIRA JR., A. C., (1994), Satellite studies of biomass burning in Amazonia – some practical aspects. *Remote Sensing Review,* **10:** 91-103.

SILVA DIAS, M. A. F. & FERREIRA, R. N., (1992), Application of a linear spectral model to the study of Amazonian squall lines. *J. Geophys. Res.*, **97** (D18): 20405-20419.

TRIPOLI, G. J. & COTTON, W. R., (1982), The Colorado State University three-dimensional cloud/mesoscale model – 1982. Part I: General theoretical framework and sensitivity experiments. *J. Res. Atmos.,* **16:** 185-219.